European Radiology (2019) 29:4258–4265
https://doi.org/10.1007/s00330-018-5908-y

ULTRASOUND

CAD system based on B-mode and color Doppler sonographic features may predict if a thyroid nodule is hot or cold

Ali Abbasian Ardakani[1,2] · Ahmad Bitarafan-Rajabi[3,4] · Afshin Mohammadi[5] · Sepideh Hekmat[6] · Aylin Tahmasebi[2] · Mohammad Bagher Shiran[2] · Ali Mohammadzadeh[7]

Received: 27 July 2018 / Revised: 25 October 2018 / Accepted: 22 November 2018 / Published online: 9 January 2019

Abstract

Objectives The aim of this study was to evaluate if the analysis of sonographic parameters could predict if a thyroid nodule was hot or cold.

Methods Overall, 102 thyroid nodules, including 51 hyperfunctioning (hot) and 51 hypofunctioning (cold) nodules, were evaluated in this study. Twelve sonographic features (i.e., seven B-mode and five Doppler features) were extracted for each nodule type. The isthmus thickness, nodule volume, echogenicity, margin, internal component, microcalcification, and halo sign features were obtained in the B-mode, while the vascularity pattern, resistive index (RI), peak systolic velocity, end diastolic velocity, and peak systolic/end diastolic velocity ratio (SDR) were determined, based on Doppler ultrasounds. All significant features were incorporated in the computer-aided diagnosis (CAD) system to classify hot and cold nodules.

Results Among all sonographic features, only isthmus thickness, nodule volume, echogenicity, RI, and SDR were significantly different between hot and cold nodules. Based on these features in the training dataset, the CAD system could classify hot and cold nodules with an area under the curve (AUC) of 0.898. Also, in the test dataset, hot and cold nodules were classified with an AUC of 0.833.

Conclusions 2D sonographic features could differentiate hot and cold thyroid nodules. The CAD system showed a great potential to achieve it automatically.

Key Points

• *Cold nodules represent higher volume ($p = 0.005$), isthmus thickness ($p = 0.035$), RI ($p = 0.020$), and SDR ($p = 0.044$) and appear hypoechogenic ($p = 0.010$) in US.*

• *Nodule volume with an AUC of 0.685 and resistive index with an AUC of 0.628 showed the highest classification potential among all B-mode and Doppler features respectively.*

• *The proposed CAD system could distinguish hot nodules from cold ones with an AUC of 0.833 (sensitivity 90.00%, specificity 70.00%, accuracy 80.00%, PPV 87.50%, and NPV 75.00%).*

Keywords Machine learning · Radionuclide imaging · Thyroid nodule · Thyrotropin · Ultrasonography, Doppler

✉ Mohammad Bagher Shiran
Shiran.m@iums.ac.ir; Shiranmb@yahoo.com

✉ Ali Mohammadzadeh
A.mohammadzadeh@rhc.ac.ir

[1] ENT and Head & Neck Research Center and Department, Hazrat Rasoul Akram Hospital, Iran University of Medical Sciences, Tehran, Iran

[2] Department of Medical Physics, School of Medicine, Iran University of Medical Sciences, Tehran, Iran

[3] Cardiovascular Intervention Research Center, Rajaie Cardiovascular Medical and Research Center, Iran University of Medical Sciences, Tehran, Iran

[4] Echocardiography Research Center, Rajaie Cardiovascular Medical and Research Center, Iran University of Medical Sciences, Tehran, Iran

[5] Department of Radiology, Faculty of Medicine, Urmia University of Medical Science, Urmia, Iran

[6] Department of Nuclear Medicine, School of Medicine, Hasheminejad Hospital, Iran University of Medical Sciences, Tehran, Iran

[7] Department of Radiology, Rajaie Cardiovascular, Medical and Research Center, Iran University of Medical Sciences, Tehran, Iran

Abbreviations

ATA	American Thyroid Association
CAD	Computer-aided diagnosis
EDV	End diastolic velocity
FNA	Fine needle aspiration
LEGP	Low-energy general purpose
PSV	Peak systolic velocity
RI	Resistive index
SDR	Peak systolic/end diastolic velocity ratio
SVM	Support vector machine
TSH	Serum thyrotropin

Introduction

Thyroid nodules can be either benign or malignant. In a report published in 2018, the National Cancer Institute estimated 53,990 new cases of thyroid cancer and 2060 deaths due to this disease [1]. Although thyroid nodules are very common, their prevalence is largely dependent on the method of detection and the studied population [2–4]. They are more common in the elderly, female populations, iodine-deficient areas, and individuals with a history of radiation exposure [5]. The prevalence of thyroid nodules detected by palpation is 4–7% in the general population, while it rises to 19–67% by ultrasound imaging [6, 7].

Ultrasonography (US) is not recommended as a screening modality for the general population [8]. The American Thyroid Association (ATA) guidelines recommend US as the primary imaging modality in patients with a thyroid nodule detected clinically or with other imaging modalities [9]. Thyroid nodule evaluation serves a critical role in identifying potentially malignant lesions and making appropriate decisions including fine needle aspiration (FNA) biopsy and treatment [10]. Based on the ATA guidelines, the level of serum thyroid-stimulating hormone (TSH) should be initially measured in patients with thyroid nodules larger than 1 cm. If the serum TSH level is subnormal, a radionuclide thyroid scan should be acquired. According to the results of radionuclide thyroid scans, nodules are classified as hyperfunctioning (hot), isofunctioning (warm), and nonfunctioning (cold) with higher, equivalent, and lower tracer uptakes, respectively, in comparison with the surrounding normal thyroid tissues. In addition, cold nodules are associated with a malignancy risk of 3–15%, and FNA biopsy is recognized as the most accurate test for the evaluation of cold thyroid nodules [9].

US features show great potential in predicting the risk of malignancy. Generally, a higher risk of malignancy is associated with the following ultrasonographic features: a taller-than-wide shape, absence of halo signs, microcalcification, irregular margins, hypoechogenicity, solid nodule components, and intranodular vascularization [8].

Computer-aided diagnosis (CAD) systems have been proposed to assist radiologists in diagnostic procedures [11, 12]. Recently, we studied the application of CAD systems in thyroid diseases and suggested it as a second-opinion interpretation or a complementary tool for diagnosis by radiologists [13–16]. An accurate and efficient CAD system for thyroid nodule classification, based on ultrasound features, should interpret data in a shorter amount of time, prevent possible medical errors, and reduce cost and patient anxiety.

In this study, we evaluated if Doppler and B-mode ultrasound features could differentiate between hot and cold nodules, and if a CAD system could achieve this distinction.

Patients and methods

Patients and image acquisition

Patients referred to Rajaie Cardiovascular Medical and Research Center for a radionuclide thyroid scan were recruited consecutively between May 2017 and March 2018. Each patient provided a written informed consent before being enrolled in the study. This prospective, cross-sectional study was also approved by the local ethics committee.

The inclusion criteria were as follows: (1) assessment of serum TSH level; (2) suppressed TSH level < 0.5 μIU/mL; and (3) presence of nodules > 10 mm in diameter. On the other hand, the exclusion criteria were as follows: (1) a recent history of myocardial infarction and surgery; (2) congestive heart failure; (3) receiving amiodarone or contrast agents; (4) pregnancy in the past 6 months; (5) suspicion of thyroiditis; and (6) having multiple nodules with a diameter of > 10 mm.

Neck US was carried out as a routine test right before the radionuclide thyroid scan. US was performed using the iU22 sonography system (Philips Healthcare), equipped with a L12-5 50-mm linear array transducer (12–5 MHz). All the detected nodules were evaluated in both longitudinal and transverse views. Also, all thyroid nodule ultrasounds were compared with the radionuclide scans for further analyses.

In this study, radionuclide thyroid scans were acquired using an Infinia Hawkeye 4SPECT-CT scanner (GE Healthcare), equipped with a low-energy general purpose (LEGP), parallel-hole collimator with a matrix size of 256 × 256 and zoom factor of two. Imaging was performed 20 min after the intravenous administration of ^{99m}Tc pertechnetate (4 mCi) for 180 s (700–1000 K counts per view). A symmetric 20% window was centered on the ^{99m}Tc 140-keV photopeak. It should be noted that all patients ceased methimazole use 1 week before the radionuclide thyroid scan to rule out this confounding factor.

Extraction of radiological features

B-mode features

Six B-mode features were extracted to characterize the nodules, namely nodule volume, echogenicity, margin, internal component, microcalcification, and halo sign. Benign thyroid nodules are usually hyperechogenic with regular margins and a solid component, without microcalcification or a hypoechoic halo [8, 17–21]. Echogenicity is classified into hypo/heteroechogenicity and hyper/isoechogenicity. Also, borders of nodules are graded as well-defined (regular) or blurred (microlobulated/irregular).

The internal component was defined as solid or mixed (both solid and cystic areas). On the other hand, isthmus thickness was measured as an anatomical feature of the thyroid gland. In order to define the size of nodules, volume was measured and defined using the ellipsoid model. Volume was calculated as follows:

$$W \times L \times T \times \pi/6 \tag{1}$$

where W, L, and T represent the width, length, and thickness of nodules, respectively.

Doppler features

Five Doppler features were extracted to characterize the nodules, including vascular pattern, resistive index (RI), peak systolic velocity (PSV), end diastolic velocity (EDV), and peak systolic/end diastolic velocity ratio (SDR). Vascularity can be classified into four categories: (1) no vascularity, absence of flow in the periphery and/or within the nodule; (2) peripheral vascularity, presence of flow only in the periphery of the nodule; (3) intranodular vascularity, presence of flow within the nodule; and (4) intranodular and peripheral vascularity, presence of flow in both the periphery and center of the nodule. All radiological features were compared with the radionuclide scan results.

Statistical analysis and classification

The Kolmogorov–Smirnov test was applied to evaluate the normal distribution of quantitative data. Two-tailed independent samples t test was used to compare the quantitative features between hot and cold thyroid nodules. To assess the distribution of radiological features and gender between the two groups, chi-square test was used. P value less than 0.05 was considered significant. Also, area under the receiver operating characteristic (ROC) curve (AUC) was calculated for each significant radiological feature to determine the overall performance of classification for hot and cold nodules.

The support vector machine (SVM) algorithm was used for all significant features to identify hot and cold nodules. Generally, SVM is a powerful supervised algorithm, used to solve classification and modeling problems in CAD systems. SVM determines the optimal hyperplane with maximum distance from each class space. In SVM, after training and building the model, new data can be assigned to one category according to the hyperplane. Cross-validation is a useful method to prevent overfitting and improve generalizability. In this study, 10-fold cross-validation was used, in which features are randomly divided into 10-folds with equal sizes. Nine folds are used for training, and 1-fold is used for testing the data. This procedure is continued until all folds are used for testing the model. Almost 80% of the subjects (50–50% distribution) were randomly selected for training, while 20% (50–50% distribution) were considered as new and blinded data to test the final model.

The classification performance of SVM was evaluated by measuring the sensitivity, specificity, accuracy, positive predictive value (PPV), negative predictive value (NPV), and AUC. In this study, hot and cold nodules were considered as negative and positive cases, respectively. SPSS version 19 was used for statistical analyses. AUC values were estimated to exceed a confidence level of 95%. Figure 1 presents the steps taken for processing the CAD system.

Results

Demographic characteristics

Overall, 12 radiological features, including seven B-mode and five Doppler features, were employed to compare the differences between hot and cold thyroid nodules. In this study, 102 patients (65 female and 37 male) with radionuclide scan–confirmed results were recruited. Among 102 patients, hot and cold nodules were each detected in 51 patients (31 female and 20 male vs. 34 female and 17 male). No significant difference was observed between the two groups of hot and cold nodules in terms of gender distribution ($p = 0.680$). Also, the mean age of patients in the hot and cold groups was 51.82 ± 12.63 and 54.83 ± 11.62 years, respectively, representing an insignificant difference ($p = 0.215$). Since the two groups were not significantly different in terms of age or gender distribution, these parameters were not considered as confounding factors.

Finally, 82 out of 102 nodules (41 hot and 41 cold nodules) were randomly selected for the training dataset, while the remaining 20 nodules (10 hot and 10 cold nodules) were considered as the new blinded data for testing the final model.

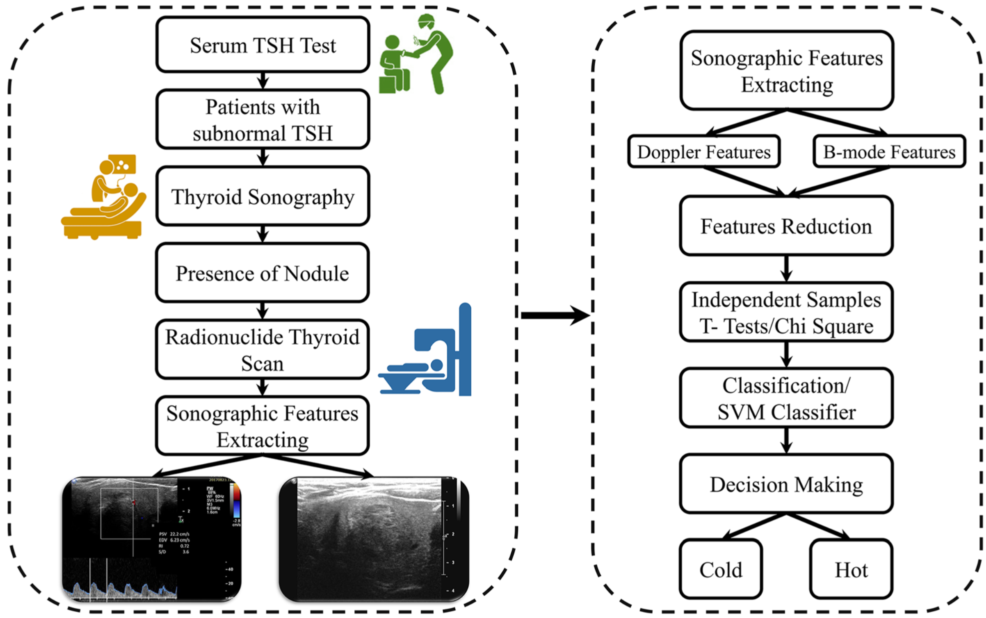

Fig. 1 Overview of the proposed CAD system process based on ultrasound image

Distribution of radiological features in the groups

The results related to B-mode and Doppler features are summarized in Tables 1 and 2, respectively. The isthmus thickness of cold nodules was significantly greater than that of hot nodules (50.36 ± 19.37 vs. 43.13 ± 14.46 mm; $p = 0.035$). Moreover, the volume of hot and cold nodules was 5.76 ± 1.99 and 7.32 ± 2.39 cm^3, respectively, which indicates a significant difference between the groups ($p = 0.005$).

Hypoechogenicity was detected in 54 (52.94%) out of 102 nodules. Also, 34 (62.96%) out of these 54 nodules indicated cold radionuclide results. On the other hand, among 48 nodules with a hyperechogenic appearance, 31 (64.58%) were hot nodules on the radionuclide scan. Therefore, hypoechogenicity was significantly more common in cold nodules, compared to that of hot nodules ($p = 0.010$). Conversely, no significant difference was observed between hot and cold nodules in terms of margin, internal component, presence of microcalcification, and halo sign ($p = 0.277$, 0.113, 0.106, and 0.109, respectively).

The RI in the cold nodule group was significantly higher than that of the hot nodule group (0.611 ± 0.12 vs. 0.552 ± 0.11; $p = 0.020$). In addition, SDR in the cold nodule group was significantly higher than that of the hot nodule group (2.89 ± 1.04 vs. 2.40 ± 0.62; $p = 0.044$). However, no significant difference was found in other Doppler indices, including PSV and EDV ($p = 0.150$ and 0.892, respectively). Similarly,

Table 1 Main ultrasound B-mode characteristics data of hot and cold thyroid nodules

B-mode parameter	Hot Mean ± SD		Cold		*p* value*
Isthmus thickness (mm)	43.13 ± 14.46		50.36 ± 19.37		0.035
Nodule volume (cm^3)	5.76 ± 1.99		7.32 ± 2.39		0.005
Echogenicity	Number (percentage)				*p* value§
	Hypo (or hetero-echo)	Hyper (or iso-echo)	Hypo (or hetero-echo)	Hyper (or iso-echo)	
	20 (39.2)	31 (60.8)	34 (66.7)	17 (33.3)	0.010
Margin	Well-defined (or regular)	Blurred (microlobulation or irregular)	Well-defined (or regular)	Blurred (microlobulation or irregular)	0.277
	39 (76.5)	12 (29.4)	33 (64.7)	18 (35.3)	
Internal component	Solid	Mix	Solid	Mix	0.113
	31 (60.8)	20 (39.2)	22 (43.1)	29 (56.9)	
Microcalcification	No	Yes	No	Yes	0.106
	35 (68.6)	16 (31.4)	26 (51.0)	25 (49.0)	
Halo echo	No	Yes	No	Yes	0.109
	17 (33.3)	34 (66.7)	26 (51.0)	25 (49.0)	

p values were obtained using *t* test (*) and chi-square test (§)

Table 2 Main Doppler ultrasound characteristics data of hot and cold thyroid nodules

Doppler parameter	Hot Mean ± SD	Cold	p value*
Resistive index (RI)	0.552 ± 0.11	0.611 ± 0.12	0.020
Peak systolic velocity (PSV)	19.04 ± 7.55	22.20 ± 12.37	0.150
End diastolic velocity (EDV)	8.63 ± 4.43	8.50 ± 4.97	0.892
Systolic/diastolic ratio (SDR)	2.40 ± 0.62	2.89 ± 1.04	0.044
Vascularity	Number (percentage)		p value§
No vascularity	6 (11.8)	8 (15.7)	0.774
Presence of vascularity	45 (88.2)	43 (84.3)	
Peripheral	13 (25.5)	18 (35.3)	0.389
Intranodular	20 (39.2)	14 (27.4)	0.294
Intranodular & Peripheral	12 (23.5)	11 (21.6)	1.000 (0.813)

p values were obtained using t test (*) and chi-square test (§)

no significant difference was observed in terms of vascular pattern between the two groups (Table 2). Figure 2 presents the B-mode and Doppler ultrasound images, as well as their corresponding scintigraphic images for hot and cold thyroid nodules.

Classification performance of hot and cold nodules

Figure 3a and Table 3 present the ROC curves and AUCs of significant radiological features, respectively. The AUCs of B-mode and Doppler parameters were within the ranges of 0.614–0.685 and 0.625–0.628, respectively. All five significant radiological features were integrated in SVM for the multiparameter analysis. Table 4 presents the diagnostic performance of SVM in classifying and comparing hot and cold nodules for the training and test datasets. SVM could distinguish hot nodules from cold ones with an AUC of 0.898 (sensitivity, 90.24%; specificity, 80.48%; and accuracy, 85.36% in the training dataset).

Using 10-fold cross-validation, the final model was tested with 20 new cases (i.e., 10 hot and 10 cold nodules). The results indicated the high performance of the model, with an AUC of 0.833, sensitivity of 90.0%, specificity of 80.0%, and accuracy of 70.0%. Figure 3b represents the ROC curves of SVM training and test models on the same graph for performance comparisons.

Discussion

The results of the present study indicated that sonographic features had great potential in differentiating between hot and cold thyroid nodules.

Nodule volume showed better differentiation between hot and cold thyroid nodules in comparison with other B-mode features. In addition, among Doppler features, RI was superior to SDR in classification of two nodule types (RI, 0.628 vs. SDR, 0.625). The AUC results indicated that the combination of B-mode and Doppler features had a higher discriminative

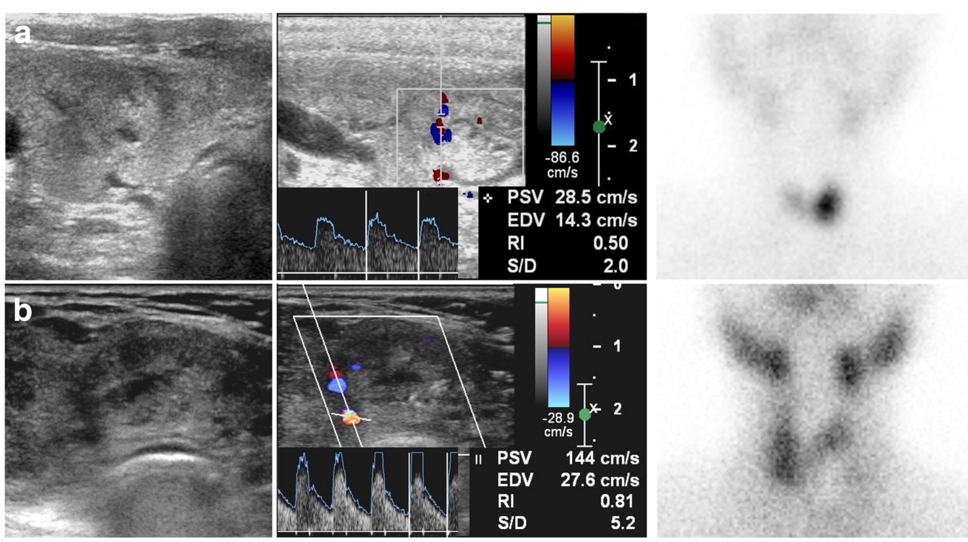

Fig. 2 Sample image of hot (**a**) and cold (**b**) nodule B-mode and color Doppler and their corresponding scintigraphic images are located at left, middle, and right of figure

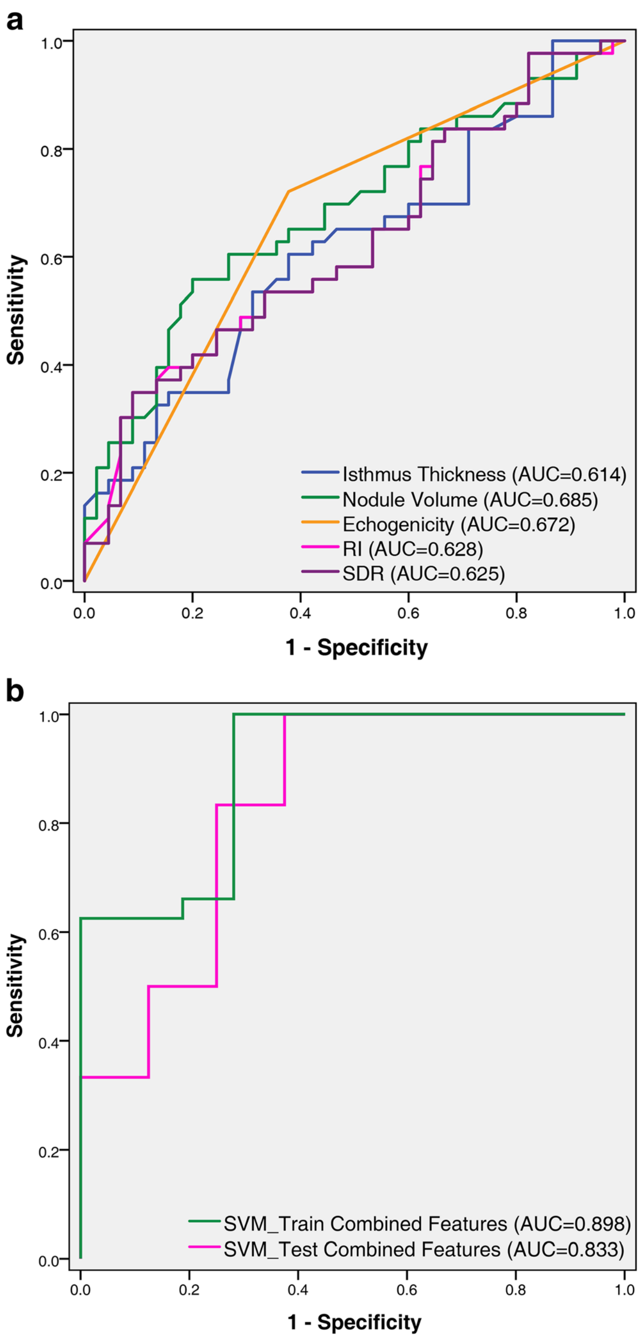

Fig. 3 ROC curves of individual significant radiological features (**a**) and combination features (**b**)

power, compared to each feature alone (combined B-mode and Doppler features vs. best B-mode feature vs. best Doppler feature, 0.898 vs. 0.685 vs. 0.628). It can be concluded that B-mode and Doppler features are complementary, and their combination can enhance performance. Moreover, the final model was tested with 20 blinded nodules (i.e., 10 hot and 10 cold nodules). Based on the findings, the model could classify the two groups with high performance (AUC, 0.833; sensitivity, 90.00%; specificity, 70.00%; and accuracy, 80.00%).

Table 3 The area under the ROC curve of significant B-mode and Doppler parameters

Parameters		AUC value*
B-mode	Isthmus thickness	0.614 (0.496, 0.732)
	Nodule volume	0.685 (0.573, 0.797)
	Echogenicity	0.672 (0.558, 0.785)
Doppler	Resistive index (RI)	0.628 (0.511, 0.745)
	Systolic/diastolic ratio (SDR)	0.625 (0.508, 0.742)

AUC area under ROC curve, *Numbers in parentheses are 95% confidence intervals

Recently, some studies have been carried out to assess different sonographic features for predicting the risk of malignancy using CAD systems. Xia et al employed an extreme learning machine system to differentiate between benign and malignant thyroid nodules, based on ultrasound images. It was found that echogenicity, margin, calcification, component, and shape were the most discriminative features. This approach showed 87.72% accuracy, 78.89% sensitivity, 94.55% specificity, and an AUC of 0.867 [22]. In another study, Moon et al evaluated the diagnostic performance of power Doppler sonography in predicting vascularity. They compared the combination of vascularity and suspicious gray-scale ultrasound features (i.e., hypoechogenicity, noncircumscribed margins, microcalcification, and a taller-than-wide shape) with gray-scale features alone in predicting thyroid nodule malignancy. Intranodular vascularity alone and combination of vascularity with suspicious gray-scale ultrasound features were less favorable in differentiating between benign and malignant thyroid nodules, compared to the combination of four suspicious gray-scale ultrasound features [23].

In addition, Choi et al compared the diagnostic performance of a CAD system with radiologists in the identification of malignant thyroid nodules on ultrasounds. The CAD system demonstrated similar sensitivity to that of radiologists (sensitivity, 90.7% vs. 88.4%), despite lower specificity and accuracy (specificity, 74.6% vs. 94.9%; AUC, 0.83 vs. 0.92). Sonographic features, including composition, orientation, echogenicity, and spongiform aspects, showed significant agreements between the radiologist and CAD system, while the margin component showed fair agreements [24]. On the other hand, Chang et al reported the slightly higher accuracy of CAD system in the diagnosis of malignancies in comparison with visual inspection by a radiologist. The accuracy and AUC of the CAD system were 98.3% and 0.986, respectively, while the accuracy and AUC of the radiologist were 94.9% and 0.979, respectively [25]. Therefore, CAD systems can help radiologists distinguish benign nodules from malignant ones.

Table 4 Diagnostic performance of the proposed radiological parameter analysis for classification of hot and cold thyroid nodules

Groups		SEN (%)	SPC (%)	ACC (%)	PPV (%)	NPV (%)	AUC value*	Correct classification
Train	Radiological features	90.24	80.48	85.36	89.19	82.22	0.898 (0.831, 0.965)	70/82 (85.36%)
Test		90.00	70.00	80.00	87.50	75.00	0.833 (0.637, 1.000)	16/20 (80.00%)

SEN sensitivity, *SPC* specificity, *ACC* accuracy, *PPV* positive predictive value, *NPV* negative predictive value, *AUC* area under ROC curve; *Numbers in parentheses are 95% confidence intervals

Additionally, in a previous study, two quantitative feature groups, including morphological and textural features, were extracted from the ultrasound images of 84 thyroid nodules (i.e., 42 hot and 42 cold nodules). The AUCs of the training and test datasets were 0.992 and 0.948, respectively [15]. The present findings are in accordance with the mentioned results and indicate that ultrasound images can help describe nodule function. Today, artificial intelligence is being increasingly used in radiology departments. The CAD system is an interesting application of artificial intelligence, with the potential to solve diagnostic problems through classification and modeling. Application of color Doppler and B-mode sonographic features in a CAD system for differentiating between hot and cold thyroid nodules is a novel idea, which requires further investigation to improve its accuracy and develop an efficient system for routine clinical practice.

This study indicated that evaluation of thyroid nodule function based on sonographic features is a promising approach, with many advantages for patients, physicians, and healthcare systems. Its benefits include real-time interpretation of sonographic results, besides reduction of the costs, radiation doses, and anxiety associated with diagnostic procedures. It also helps radiologists, endocrinologists, and surgeons to determine the risk of malignancy and select proper thyroid nodule treatment plans. In addition, this approach eliminates unnecessary tests and facilitates patient referral for surveillance programs.

Further research is required to corroborate our findings and improve the accuracy of sonographic features in characterizing thyroid nodules for routine clinical practice. It should be noted that patients with warm (isofunctioning) nodules were not included in this study. This study was a preliminary attempt to evaluate the potential of US in classifying hot and cold nodules. Therefore, further investigations should be undertaken on all types of nodules to obtain comprehensive results. It should be also noted that Doppler angle can affect velocity measurements; in fact, a small angle can increase velocity unrealistically. One of the limitations of this study is that we could not use a correct Doppler angle for all the samples. However, RI and SDR are generally independent of angle, and consequently, the results based on these two parameters are reliable. In addition, use of an incorrect angle may be the main reason why PSV and EDV are not significantly different between the groups.

Conclusion

In conclusion, a CAD system based on B-mode and Doppler sonographic features seems to be a useful complementary tool for the evaluation of nodule function in diagnostic procedures during radionuclide imaging. In addition, it can help radiologists improve their understanding of conventional thyroid US.

Funding This study has received funding from the Iran University of Medical Sciences.

Compliance with ethical standards

Guarantor The scientific guarantor of this publication is Mohammad Bagher Shiran.

Conflict of interest The authors of this manuscript declare no relationships with any companies, whose products or services may be related to the subject matter of the article.

Statistics and biometry One of the authors has significant statistical expertise.

Informed consent Written informed consent was obtained from all subjects (patients) in this study.

Ethical approval Institutional Review Board approval was not required because all diagnostic procedures were performed according to American thyroid association (ATA).

This study was approved by the ethics committee of the Iran University of Medical Sciences (No. IR.IUMS.REC 1395.95-04-30-29762).

Methodology
• prospective

Publisher's Note Springer Nature remains neutral with regard to jurisdictional claims inpublished maps and institutional affiliations.

References

1. National Cancer Institute. Thyroid cancer—patient version. Available via http://www.cancer.gov/cancertopics/types/thyroid. Accessed 25 Jul 2018
2. Tan GH, Gharib H, Reading CC (1995) Solitary thyroid nodule. Comparison between palpation and ultrasonography. Arch Intern Med 155:2418–2423

3. Reiners C, Wegscheider K, Schicha H et al (2004) Prevalence of thyroid disorders in the working population of Germany: ultrasonography screening in 96,278 unselected employees. Thyroid 14: 926–932
4. Guth S, Theune U, Aberle J, Galach A, Bamberger CM (2009) Very high prevalence of thyroid nodules detected by high frequency (13 MHz) ultrasound examination. Eur J Clin Invest 39:699–706
5. Dean D, Gharib H (2008) Epidemiology of thyroid nodules. Best Pract Res Clin Endocrinol Metab 22:901–911
6. Tan G, Gharib H (1997) Thyroid incidentalomas: management approaches to nonpalpable nodules discovered incidentally on thyroid imaging. Ann Intern Med 126:226–231
7. Bartolotta T, Midiri M, Runza G et al (2006) Incidentally discovered thyroid nodules: incidence, and greyscale and colour Doppler pattern in an adult population screened by real-time compound spatial sonography. Radiol Med 111:989–998
8. Gharib H, Papini E, Garber J et al (2016) American Association of Clinical Endocrinologists, American College of Endocrinology, and Associazione Medici Endocrinologi medical guidelines for clinical practice for the diagnosis and management of thyroid nodules–2016 update. Endocr Pract 22:622–639
9. Haugen BR, Alexander EK, Bible KC et al (2016) American Thyroid Association management guidelines for adult patients with thyroid nodules and differentiated thyroid cancer: the American Thyroid Association guidelines task force on thyroid nodules and differentiated thyroid cancer. Thyroid 26:1–133
10. Frates M, Benson C, Doubilet P et al (2006) Prevalence and distribution of carcinoma in patients with solitary and multiple thyroid nodules on sonography. J Clin Endocrinol Metab 91:3411–3417
11. van Ginneken B, Schaefer-Prokop C, Prokop M (2011) Computer-aided diagnosis: how to move from the laboratory to the clinic. Radiology 261:719–732
12. Takahashi R, Kajikawa Y (2017) Computer-aided diagnosis: a survey with bibliometric analysis. Int J Med Inform 101:58–67
13. Abbasian Ardakani A, Gharbali A, Mohammadi A (2015) Application of texture analysis method for classification of benign and malignant thyroid nodules in ultrasound images. Iran J Cancer Prev 8:116–124
14. Abbasian Ardakani A, Gharbali A (2015) Classification of benign and malignant thyroid nodules using wavelet texture analysis of sonograms. J Ultrasound Med 34:1983–1989
15. Ardakani AA, Mohammadzadeh A, Yaghoubi N et al (2018) Predictive quantitative sonographic features on classification of hot and cold thyroid nodules. Eur J Radiol 101:170–177
16. Abbasian Ardakani A, Reiazi R, Mohammadi A (2018) A clinical decision support system using ultrasound textures and radiologic features to distinguish metastasis from tumor-free cervical lymph nodes in patients with papillary thyroid carcinoma. J Ultrasound Med 37:2527–2535
17. Moon WJ, Jung SL, Lee JH et al (2008) Benign and malignant thyroid nodules: US differentiation–multicenter retrospective study. Radiology 247(3):762–770
18. Ma JJ, Ding H, Xu BH et al (2014) Diagnostic performances of various gray-scale, color Doppler, and contrast-enhanced ultrasonography findings in predicting malignant thyroid nodules. Thyroid 24:355–363
19. Roman SA, Sosa JA, Solórzano CC (2017) Management of thyroid nodules and differentiated thyroid cancer: a practical guide. Springer International Publishing, Cham. https://doi.org/10.1007/978-3-319-43618-0
20. Wu H, Deng Z, Zhang B, Liu Q, Chen J (2016) Classifier model based on machine learning algorithms: application to differential diagnosis of suspicious thyroid nodules via sonography. AJR Am J Roentgenol 207:859–864
21. Xu SY, Zhan WW, Wang WJ (2015) Evaluation of thyroid nodules by a scoring and categorizing method based on sonographic features. J Ultrasound Med 34:2179–2185
22. Xia J, Chen H, Li Q et al (2017) Ultrasound-based differentiation of malignant and benign thyroid nodules: an extreme learning machine approach. Comput Methods Programs Biomed 147:37–49
23. Moon HJ, Kwak JY, Kim MJ, Son EJ, Kim EK (2010) Can vascularity at power Doppler US help predict thyroid malignancy? Radiology 255:260–269
24. Choi YJ, Baek JH, Park HS et al (2017) A computer-aided diagnosis system using artificial intelligence for the diagnosis and characterization of thyroid nodules on ultrasound: initial clinical assessment. Thyroid 27:546–552
25. Chang Y, Paul AK, Kim N et al (2016) Computer-aided diagnosis for classifying benign versus malignant thyroid nodules based on ultrasound images: a comparison with radiologist-based assessments. Med Phys 43:554–567